Root cap cell corpse clearance limits microbial colonization in *Arabidopsis thaliana*

Nyasha M. Charura[1+], Ernesto Llamas[1+], Concetta De Quattro[1], David Vilchez[2,3,4], Moritz K. Nowack[5,6#] and Alga Zuccaro[1#*]

[1] Cluster of Excellence on Plant Sciences (CEPLAS), Institute for Plant Sciences, University of Cologne, D-50674 Cologne, Germany.

[2] Cologne Excellence Cluster for Cellular Stress Responses in Aging-Associated Diseases (CECAD), University of Cologne, 50931 Cologne, Germany.

[3] Center for Molecular Medicine Cologne (CMMC), University of Cologne, 50931 Cologne, Germany.

[4] Faculty of Medicine, University Hospital Cologne, 50931 Cologne, Germany.

[5] Department of Plant Biotechnology and Bioinformatics, Ghent University, 9052 Ghent, Belgium

[6] VIB Center for Plant Systems Biology, 9052 Ghent, Belgium

[#]shared last author

[+]shared first author

*Corresponding author: azuccaro@uni-koeln.de

Abstract

Developmental programmed cell death (dPCD) in *Arabidopsis thaliana* is an integral part of the differentiation process of the root cap, a specialized organ surrounding meristematic stem cells. dPCD in lateral root cap (LRC) cells depends on the transcription factor ANAC033/SOMBRERO (SMB) and is followed by rapid cell-autonomous corpse clearance, involving the senescence-associated nuclease BFN1 downstream of SMB. Based on transcriptomic analyses, we observed the downregulation of *BFN1* during colonization of *A. thaliana* by the beneficial root endophyte *Serendipita indica*. Roots of *smb3* mutants, deficient in root cap dPCD and corpse clearance, are covered by uncleared LRC cell corpses and hypercolonized by *S. indica* from the root tip upwards. The *bfn1-1* mutant exhibits an attenuated delayed corpse clearance phenotype, but still enhances colonization by *S. indica*. These results highlight that the constant production

and clearance of LRC cells, in addition to its function in root cap size control, represents a sophisticated physical defense mechanism to prevent microbial colonization in close proximity to meristematic stem cells. Furthermore, we propose a mechanism by which *S. indica* manipulates dPCD in *A. thaliana* roots by downregulating *BFN1* to promote fungal colonization through delayed clearance of dead cells, which present potential sources of nutrients.

Keywords

Programmed cell death (PCD) / developmental PCD (dPCD) / root cap / lateral root cap (LRC) / SOMBRERO (SMB) / plant-microbe interaction / root colonization / *Serendipita indica* / root cell corpses / root stem cells / BFN1

Introduction

Plant roots elongate by producing new cells in the meristematic tissue at the apical region of root tips. As roots extend further into the soil environment, the newly formed root tissue is naturally exposed to microbial attacks, which poses a challenge to the successful establishment of root systems. However, microbial colonization of the meristematic zone in root tips is rarely detected (Deshmukh *et al.*, 2006, Jacobs *et al.*, 2011). The sensitive tissue of the apical root meristem is surrounded by the root cap, a specialized root organ that orchestrates root architecture, directs root growth based on gravitropism and hydrotropism, and senses environmental stimuli (Kumpf & Nowack, 2015, Moriwaki *et al.*, 2013). In addition, the root cap is presumed to have a protective function in the exploration of the soil by the roots (Kumpf & Nowack, 2015, Moriwaki *et al.*, 2013).

In *Arabidopsis thaliana* (hereafter Arabidopsis), the root cap consists of two distinct tissues: the centrally located columella root cap at the very root tip and the peripherally located lateral root cap (LRC), which flanks both the columella and the entire root meristem (Dolan *et al.*, 1993). A ring of specific stem cells continuously generates both new LRC cells and root epidermis cells (Dolan et al., 1993). However, despite the constant production of LRC cells, the root cap itself does not grow in size but matches the size of the meristem (Fendrych *et al.*, 2014, Barlow, 2002, Kumpf & Nowack, 2015). To maintain size homeostasis, root cap development is a highly regulated process that

varies in different plant species. In Arabidopsis, a combination of developmental programmed cell death (dPCD) and shedding of old cells into the rhizosphere has been described (Bennett *et al.*, 2010, Kumpf & Nowack, 2015). The centrally located columella root cap is shed as a cell package into the rhizosphere along with adjacent proximal LRC cells, followed by a PCD process happening in the rhizosphere (Shi *et al.*, 2018, Feng *et al.*, 2022, Huysmans *et al.*, 2018). In contrast, LRC cells in the upper part of the root tip elongate and reach the distal edge of the meristem where they undergo dPCD orchestrated by the root cap-specific transcription factor ANAC33/SOMBRERO (SMB) (Fendrych et al., 2014, Willemsen *et al.*, 2008, Bennett et al., 2010). SMB belongs to a plant-specific family of transcription factors carrying a NAC domain (NAM - no apical meristem; ATAF1 and −2, and CUC2 - cup-shaped cotyledon). In the root cap, SMB promotes the expression of genes involved in the initiation and execution of LRC cell death, including the senescence-associated, bifunctional nuclease *BFN1* (Huysmans et al., 2018). BFN1 is compartmentalized in the ER and released into the cytoplasm during dPCD to exert its enzymatic activity on nucleic acids in dying cells (Reza *et al.*, 2018, Fendrych et al., 2014). Cytosolic and nuclear DNA and RNA fragmentation, as part of a rapid cell-autonomous corpse clearance on the root surface, is delayed in *bfn1-1* loss-of-function mutants (Fendrych et al., 2014). Precise timing of cell death and elimination of LRC cells before they fully enter the root elongation zone is essential for maintaining root cap size and optimal root growth (Fendrych et al., 2014). Loss of SMB activity results in a delayed cell death, causing LRC cells to enter the elongation zone where they eventually die without expression of dPCD-associated genes in the root cap, such as *BFN1* and *PASPA3* (Olvera-Carrillo et al., 2015). Interestingly, the aberrant cell death of LRC cells in the elongation zone of *smb3* mutants is not followed by corpse clearance, resulting in an accumulation of uncleared cell corpses along the entire root surface (Fendrych et al., 2014).

Despite its importance in root morphology and plant development, little is known about the impact of impaired dPCD in the root cap on plant-microbe interactions. To address the link between fungal accommodation and plant developmental cell death, we analyzed transcriptomic data and observed downregulation of *BFN1* in Arabidopsis during colonization by *Serendipita indica*, a beneficial fungus of the order Sebacinales. As a root

endophyte, *S. indica* colonizes the epidermal and cortex layers of a broad range of different plant hosts, conferring various beneficial effects, including plant growth promotion, protection against pathogenic microbes and increased tolerance to abiotic stresses (Boorboori & Zhang, 2022, Mahdi *et al.*, 2022, Fesel & Zuccaro, 2016). The colonization strategy of *S. indica* comprises an initial biotrophic interaction between plant and fungus. Once established in its plant host, *S. indica* enters a growth phase associated with a restricted host cell death that does not, however, diminish the beneficial effects on the plant host. The induction of restricted cell death in the epidermal and cortex layers of roots is a crucial component of the colonization strategy of *S. indica* and is accompanied by increased production of fungal hydrolytic enzymes (Zuccaro *et al.*, 2011, Deshmukh et al., 2006). Although several effector proteins involved in fungal accommodation have been described (Dunken *et al.*, 2022, Weiss *et al.*, 2016), the exact mechanism by which *S. indica* manipulates cell death in plants is still unclear.

Here we show that the bifunctional nuclease *BFN1,* involved in dPCD processes including LRC corpse clearance, is downregulated in Arabidopsis roots during colonization by *S. indica*, which led us to investigate loss-of-function mutants of BFN1 and its upstream transcriptional regulator SMB. *smb3* mutant plants accumulate uncleared LRC cell corpses, which surround the root and enhance *S. indica* attachment and colonization along the entire root axis, even in the root tip where colonization does not normally occur in wild-type (WT) plants. Furthermore, we show that *S. indica* clears dead LRC cells of *smb3* mutant plants, most likely by degradation and uptake of nutrients from the cell corpses. Similarly, we observe that the *bfn1-1* mutants also enhance fungal colonization, despite a less pronounced delayed corpse clearance phenotype and accumulation of undegraded cells. Both mutants are characterized by the accumulation of protein aggregates in dead and dying cells. Taken together, our data demonstrate that tight regulation of host dPCD and rapid and complete root cap clearance play important roles in restricting fungal colonization. Manipulation of dPCD by downregulating *BFN1* during colonization may therefore provide a means to enhance fungal accommodation and nutrient availability to the fungus.

Results

BFN1, **a downstream component of dPCD involved in cell corpse clearance**, **is downregulated during interaction with *S. indica***

dPCD is the final step of LRC differentiation to maintain root cap organ size in the root tip of Arabidopsis. This process is orchestrated by the transcription factor SMB and executed by its direct and indirect downstream targets, including the nuclease BFN1. To explore the role of root dPCD during *S. indica* accommodation in Arabidopsis, we performed transcriptional analyses to track changes in the expression profile of cell death marker genes during different colonization stages. The major regulator of LRC cell death, the transcription factor *SMB*, showed no changes in expression during fungal colonization (**Fig**. **1A, B**). However, a marked decrease in the expression of the senescence-associated nuclease *BFN1* was observed at 6 days post inoculation (dpi), a time point that correlates with the onset of cell death by *S. indica* in Arabidopsis (**Fig. 1A, B**). To validate the RNA-Seq analysis, we performed quantitative real time-PCR (qRT-PCR), confirming *BFN1* downregulation at the onset of cell death in *S. indica*-colonized plants (**Fig. 1C**).

Induction of dPCD triggers the release of BFN1 from the ER into the cytoplasm, where irreversible fragmentation of cytosolic and nuclear DNA and RNA occurs as part of the clearing of cell corpses (Fendrych et al., 2014). It has previously been shown that the roots of the *bfn1-1* T-DNA insertion KO mutant line exhibit delayed nuclear degradation during corpse clearance (Fendrych et al., 2014, Huysmans et al., 2018) (**Fig. 1D**). Accordingly, staining with Evans blue, a viability dye that penetrates non-viable and damaged cells (Vijayaraghavareddy et al., 2017), showed an increase in cellular remnants on the *bfn1-1* epidermal cell layer at the transition between the elongation and differentiation zones (**Fig. 1E, F and Fig. S8**). These results are consistent with the proposed involvement of BFN1 in cell corpse clearance during dPCD in the Arabidopsis root cap.

We further characterized the *bfn1-1* mutant with Proteostat, a fluorescent dye that binds to quaternary protein structures typically found in misfolded and aggregated proteins (Llamas *et al.*, 2021). In WT root tips, we have previously observed that protein aggregates accumulate during root differentiation in dying and sloughed columella cell

packages but not in young LRC and meristematic cells or healthy differentiated cells (Llamas et al., 2021). While the roots of WT Arabidopsis plants were devoid of Proteostat signal, the *bfn1-1* mutant exhibited staining along the root axis, starting at the transition between elongation and differentiation zone. The meristematic root tip zone remained free of the Proteostat signal and thus free from misfolded proteins and protein aggregates (**Fig. 1G, H and Fig. S1**). These data suggest that the lack of BFN1 activity affects protein homeostasis (proteostasis) and folding in Arabidopsis roots.

To investigate the role of BFN1 in *S. indica* root colonization, we quantified extraradical colonization of *S. indica*-inoculated *bfn1-1* and WT seedlings by comparing the staining intensities of the chitin-binding fluorescent marker Alexa Fluor 488 conjugated to Wheat Germ Agglutinin (WGA-AF 488). The *bfn1-1* mutant exhibited significantly stronger staining, indicating higher extraradical colonization than in WT Arabidopsis. (**Fig. 2A-C and Fig. S2**). Quantification of intraradical colonization by qRT-PCR after careful removal of outer fungal hyphae, showed increased *S. indica* colonization in the *bfn1-1* mutant at later stages of interaction (**Fig. 2D**). Together, these results suggest that downregulation of *BFN1* during colonization is beneficial for intra- and extraradical fungal accommodation.

SMB is involved in restricting fungal colonization

To better characterize the role of disrupted dPCD in Arabidopsis LRCs, we analyzed the effect of a loss-of-function mutation in the transcription factor SMB, a key element of LRC differentiation and upstream regulator of BFN1 (**Fig. 1D**). The extent of cell death in the *smb3* T-DNA insertion line could be visualized with Evans blue staining, which highlighted the presence of uncleared LRC cell corpses along the entire surface of *smb3* roots, starting right after the meristematic zone (**Fig. 3A, B and Fig. S4**). Proteostat staining revealed an accumulation of misfolded and aggregated proteins in the uncleared dead LRC cells adhering to the roots of *smb3* (**Fig. 3C, D, E**). However, neither Proteostat signal nor Evans blue staining was detected in young LRC cells covering the meristem or in cells beneath the uncleared dead LRC cells (**Fig. 3 C, D, E and Fig. S4**). Filter trap analyses confirmed that more protein aggregates were present in *smb3* roots compared

to WT roots (**Fig. 3F**). These data suggest that the accumulation of protein aggregates in *smb3* LRC cell corpses occurs when they unintentionally enter the elongation zone.

To assess extracellular fungal colonization, we quantified WGA-AF 488 signal in *S. indica*-inoculated *smb3* and WT seedlings. *S. indica* showed a preferential colonization of the differentiation zone of WT roots and exhibited a significant increase in fungal growth on *smb3* roots along the entire root axis (**Fig. 4A, B**). Interestingly, *S. indica* also grew around the root tip of *smb3* seedlings, colonizing the meristematic zone of the root apex (**Fig. 4A and 5A**), a region normally not associated with microbial colonization (Deshmukh et al., 2006, Jacobs et al., 2011). The intraradical biomass of *S. indica* was also consistently increased in *smb3* compared to WT roots (**Fig. 4C**). Cytological analysis by confocal laser scanning microscopy (CLSM) confirmed that *S. indica* does not colonize the root tip of WT plants, but preferentially colonizes the mature parts of the root, corresponding to the differentiation zone (**Fig. 5A, C**). We also observed that *S. indica* accommodates in cells that are subject to cell death and protein aggregation (**Fig. 5**). Thus, these data indicate that uncleared LRC cell corpses in *smb3* appear to function like a scaffold for fungal colonization even at the root tip and that continuous clearance of root cap cells is likely a mechanism to prevent microbial colonization of the root tip.

To assess whether *S. indica* is able to digest the accumulating root cap cell corpses in the *smb3* mutant, we compared Evans blue staining for cell death detection of colonized and uncolonized roots. While mock-inoculated *smb3* roots displayed an accumulation of Evans blue stained LRC cell corpses, *smb3* roots colonized with *S. indica* were cleared of the excess dead LRC cells (**Fig. 5F and Fig. S9**). These results indicate that the surplus of cell corpses in *smb3* promotes colonization by *S. indica*.

Cell non-autonomous activation of cell death by *S. indica*

In Arabidopsis WT roots, dPCD execution and corpse clearance orchestrated by the transcription factor SMB and the nuclease BFN1 prevents unintended accumulation of LRC cell corpses upstream of the meristem (Fendrych et al., 2014). Based on the observation that *S. indica* downregulates *BFN1*, we hypothesized that such downregulation leads to a reduced rate of cell corpse clearance in WT roots, which positively affects *S. indica* by serving as potential additional sources of nutrients. To test

this hypothesis, we performed cell death analyses with WT Arabidopsis roots inoculated with *S. indica*. Evans blue staining revealed a pattern of dead cells originating at the onset of the differentiation zone, similar to the *bfn1-1* cell death phenotype (**Fig. 6A, B**). These results suggest an intrinsic activation of cell death by *S. indica* in this part of the root. Interestingly, we noticed further similarities between the phenotype of the *bfn1-1* mutant and WT roots colonized by *S. indica*. Measurements of root length from the tip to the first hairs highlighted that the elongation zone is shorter upon *S. indica* colonization than in mock WT roots (**Fig. 6C and Fig. S6, S8**). Moreover, Proteostat staining in *S. indica*-colonized roots occurred along the entire root axis, starting from the onset of the differentiation zone, as we observed in *bfn1-1* (**Fig. 6D and Fig. S1, S3**). Our results suggest that *S. indica* affects dPCD by reducing proteostasis and LRC clearance in Arabidopsis root caps in a non-cell autonomous manner.

To determine whether other beneficial microbes affect dPCD by downregulating *BFN1*, we analyzed the transcriptional response of Arabidopsis roots colonized by *S. vermifera*, an orchid mycorrhizal fungus closely related to *S. indica*, and two bacterial synthetic communities (SynComs) isolated from Arabidopsis or *Hordeum vulgare* (Mahdi et al., 2022). *BFN1* levels were reduced in Arabidopsis roots during all three microbial interactions (**Fig. 7**). Furthermore, similar to *S. indica*, the interaction of *S. vermifera* with Arabidopsis led to an induction of cell death in the differentiated root tissues and to a shorter elongation zone (**Fig. S5, S7**). These results suggest that beneficial microbes may have evolved the ability to manipulate dPCD and root cap turnover to increase symbiotic colonization (**Fig. 8**).

Discussion

Impaired dPCD affects plant-microbe interactions

Developmental cell death in plants and animals is a process critical for differentiation and homeostasis. As new tissue grows, old tissue must be disposed of to maintain healthy homeostasis at cellular and systemic levels. Examples of dPCD in plants can be found in xylem development, where controlled cell death forms cavities for water transport or in lateral root formation, which is facilitated by restricted cell death in cell layers above developing root primordia (Escamez *et al.*, 2020, Heo *et al.*, 2017). As a plant organ that

continuously produces new tissues but maintains a fixed size, the root cap is characterized by high cellular turnover (Kumpf and Nowack, 2015). Such cellular turnover in LRCs of Arabidopsis roots is controlled by the transcription factor SMB and downstream by the nuclease BFN1 (Fendrych et al., 2014). Despite its importance in plant health and development, little attention has been paid to the influence of dPCD on accommodation of microbes and *vice versa*.

In this study, we investigated the functional link between dPCD processes and microbial accommodation by characterizing *smb3* and *bfn1-1* Arabidopsis mutants during fungal interaction. We found that interference with dPCD and corpse clearance in the root cap, has implications for the entire root system, with some nuanced differences. While *smb3* roots are sheathed with uncleared dead LRC cells starting from the elongation zone, the epidermal cell layer beneath does not seem to be affected (**Fig. S4**). In *bfn1-1* roots we observed dead cells at the onset of the differentiation zone. Here, it remains unclear whether these cells originate from the root cap or are epidermal cells (**Fig. 1E, F and 3A, B**). Both *smb3* and *bfn1-1* mutations are characterized by increased protein misfolding and aggregation. However, while the presence of protein aggregates in *smb3* is clearly restricted to dead LRC cells and correlates with Evans blue staining, the epidermal cell layer of *bfn1-1* is littered with misfolded proteins and aggregates along the root axis starting from the differentiation zone, regardless of the occurrence of cell death. These data suggest that in the root of Arabidopsis, BFN1 activity is not limited to its proposed function in eliminating LRC cell corpses, but has potential ties to cellular stress signaling and cell death in the differentiation zone. It was recently demonstrated that small active metabolites can modulate cell death (Yu *et al.*, 2022). In plants, the Toll/interleukin-1 receptor (TIR) domains of nucleotide-binding leucine rich repeat (NLR) immunoreceptors possess NADase enzymatic activity, as well as 2′,3′-cAMP/cGMP synthetases activity by hydrolyzing RNA/DNA (Duxbury *et al.*, 2020, Yu et al., 2022). While NADase activity is not sufficient to induce plant immune responses, mutations that specifically disrupt synthetase activity abolish TIR-mediated cell death in *Nicotiana benthamiana*, demonstrating that cNMPs (cyclic nucleotide monophosphates) play an important role in TIR immune signaling. Also it was shown that the combined activity of two fungal apoplastic enzymes, the ecto-5'-nucleotidase E5NT and the nuclease NucA from *S.*

indica, leads to the production of deoxyadenosine (dAdo), a metabolite that, upon uptake, triggers a TIR-NLR-modulated plant cell death (Dunken et al., 2022). These results suggest that the DNAse activity of BFN1 may be involved in the production of small active metabolites in the plant that might affect, on different levels, cell death, proteostasis and plant-microbe interactions. Differential modulation of potential infochemicals in the *bfn1-1* mutant could therefore delay cellular damage signaling and cause protein misfolding and aggregation, a hypothesis that should be further analyzed by metabolomic and proteomic approaches.

To investigate the role of dPCD in the root cap during interaction with plant microbes, we assayed intra- and extraradical colonization with the endophytic fungus *S. indica* in *bfn1-1* and *smb3* mutants (**Fig. 2 and 4**). Both approaches show that attenuation or loss of corpse clearance in the root cap increases fungal colonization. Based on the observation that *S. indica* is able to clear the LRC cell corpses on *smb3* roots, it is conceivable that the uncleared LRC cells provide an additional source of nutrients that promote overall fungal growth. Whether production of the above-described dAdo by *S. indica* potentially influences dPCD remains to be tested.

In WT plants, the root tip is usually free of microbial colonization (Deshmukh et al., 2006, Jacobs et al., 2011). Interestingly, we detected significant fungal colonization around the root tip of *smb3*, but not *bfn1-1* or WT plants. Cytological analyses have shown that *S. indica* grows in detached, dead cell packages of LRC and columella cells, but rarely in WT root tips (Dunken et al., 2022, Deshmukh et al., 2006). The phenotype of *smb3* shows resemblance to the human skin disease hyperkeratosis. In healthy human skin, a pool of stem cells produces layers of cells that divide, differentiate, die, and are shed. Such developmental programs form a physical and dynamic barrier. When microbes attempt to establish themselves in the skin, they are consistently removed by skin exfoliation (Dettmer, 2021). Patients with hyperkeratosis show an accumulation of dead cells on the outer layer of their skin, making it more susceptible to microbial infection (Cheng *et al.*, 1992). Our results suggest that root cap turnover in Arabidopsis, similar to human skin turnover, may be a sophisticated physical mechanism to prevent or reduce intracellular microbial colonization near the root meristematic tissue. In contrast, despite the delayed

clearance phenotype, *bfn1-1* does not appear to accumulate additional root cap layers and thus preventing fungal accommodation in the root tip.

Together, we demonstrate that proper root cap development, including cell death and cell clearance, influences plant-microbe interactions and is important for restricting microbial colonization in the root tip (**Fig. 8**).

Microbial manipulation of developmental cell death

The root cap is thought to be associated with protection of the underlying meristematic stem cells (Kumar & Iyer-Pascuzzi, 2020). Previous studies have highlighted the importance of the root cap in plant-microbe interactions, for example the physical removal of the root cap in maize plants leads to increased colonization of the root tip by *Pseudomonas fluorescens* (Humphris *et al.*, 2005). However, little is known about the impact of microbial colonization on plant dPCD. Here, we propose that microbes affect dPCD and corpse clearance in the root cap of Arabidopsis by downregulating the nuclease *BFN1*.

Many features of the root phenotype induced by *S. indica* colonization show striking similarities to the root phenotype of the *bfn1-1* mutant. These similarities include the cell death pattern in differentiated root tissue, which might be a remnant of delayed LRC corpse clearance and promotes fungal growth. Furthermore, we observed a shortened elongation zone, for which we cannot discriminate whether it is due to an effect on cell division, cell elongation or a systemic effect on the whole root tip zone leading to an earlier onset of the root hair zone. Interestingly, we detected a shortening of the elongation zone in Arabidopsis colonized by *Serendipita vermifera*, which also downregulates *BFN1*. Concerning the increased protein aggregation in *bfn1-1* and *S. indica*-colonized WT roots, it is still unknown whether *S. indica*-induced protein misfolding and aggregation is directly or indirectly linked to *BFN1* downregulation or whether other components contribute to this phenotype. However, the similarities in *bfn1-1* and *S. indica*-induced phenotypes suggest that the biphasic colonization strategy of *S. indica* in Arabidopsis may be related to the temporal downregulation of the nuclease activity of BFN1 and thus to the manipulation of dPCD in the root cap.

The mechanism underlying *BFN1* downregulation by *S. indica* remains to be investigated. It is unclear whether an active interference by fungal effector proteins and signaling molecules or a systemic response of Arabidopsis occurs in the presence of *S. indica*. Previous studies have shown that *S. indica* preferentially colonizes roots in the mature differentiation zone, but we also observed a cell death pattern at the onset of the differentiation tissue near the root tip. Therefore, we suggest that active downregulation by effector proteins is unlikely due to the spatial separation of the two zones (**Fig. 6**). In addition, we have shown that other beneficial microbes such as the closely related fungus *S. vermifera* and two synthetic bacterial communities isolated from Arabidopsis and *Hordeum vulgare* (Mahdi et al., 2022) also downregulate *BFN1* during Arabidopsis colonization. These results highlight the possibility of a conserved systemic response of Arabidopsis to beneficial microbes that involves the downregulation of *BFN1* to facilitate symbiotic interactions. It remains to be clarified whether this applies only to beneficial or also to pathogenic microbes. Unlike *SMB*, *BFN1* expression in Arabidopsis is not restricted to the root cap, but can also be found in cells adjacent to emerging lateral root primordia, in differentiating xylem tracheary elements, as well as in senescent leaves, and in the abscission zones of flowers and seeds (Farage-Barhom *et al.*, 2008, Escamez et al., 2020). Therefore, future studies should clarify whether downregulation of senescence-associated *BFN1* in Arabidopsis roots by microbes occurs locally in the root cap as part of SMB-induced cell death or also as part of developmental cell death processes in the differentiation zone.

In conclusion, our data indicate that tight regulation of host dPCD and proper root cap clearance play an important role in restricting fungal colonization. However, microbes may have evolved strategies to manipulate dPCD and root cap turnover, to promote symbiotic colonization in dying root cells (**Fig. 8**).

Materials and methods

Fungal strains and growth conditions

Fungal experiments were performed with *Serendipita indica* strain DSM11827 (German Collection of Microorganisms and Cell Cultures, Braunschweig, Germany). *S. indica* was grown on complete medium (CM) containing 2% (w/v) glucose and 1.5% (w/v) agar

(Hilbert et al., 2012). Fungal material was grown at 28°C in the dark for 4 weeks before spore preparation.

For additional experiments, fungal strain *Serendipita vermifera* (MAFF305830) was used and grown on MYP medium containing 1.5% agar at 28°C in darkness for 3 weeks before mycelium preparation for root inoculation.

Plant material and growth conditions

Seeds of *Arabidopsis thaliana* ecotype Columbia 0 (Col-0) and T-DNA insertion mutants (*bfn1-1* [GK-197G12] and *smb3* [SALK_143526C]) in Col-0 background were used for experiments.

Seeds were surface sterilized in 70% ethanol for 15 min and 100% ethanol for 12 min, stratified at 4°C in the dark for 3 days and germinated and grown on ½ MS medium (Murashige-Skoog Medium, with vitamins, pH 5.7) containing 1% (w/v) sucrose and 0.4% (w/v) Gelrite under short-day conditions (8 h light, 16 h dark) with 130 µmol m^{-2} s^{-1} light and 22°C/18 °C.

Fungal inoculation

One-week-old seedlings were transferred to 1/10 PNM (Plant Nutrition Medium, pH 5.7) plates without sucrose, using 15 to 20 seedlings per plate. Under sterile conditions, chlamydospores of *S. indica* were scraped from solid CM plates in 0.002% Tween water (Roth), washed two times with ddH_2O and pipetted in a volume of 2 ml directly on plant roots and surrounding area in a concentration of $5x10^5$ per plate. ddH_2O was used for inoculation of mock plants. Unless otherwise indicated, plants were treated using this inoculation protocol. Where indicated, we also inoculated Arabidopsis seeds with *S. indica*. For this case, Arabidopsis seeds were surface sterilized, incubated with fungal spore solution at $5x10^5$ concentration for 1 hour and plated on ½ MS plates (without sucrose).

For *S. vermifera* inoculation, mycelium was scrapped from plates in ddH_2O, washed and added to Arabidopsis roots in a volume of 1 ml of a stock solution of 1 g / 50 ml.

Evans blue staining

For the visualization of cell death in Arabidopsis roots a modified protocol by (Vijayaraghavareddy *et al.*, 2017) was used. Roots were washed three times in ddH_2O to remove lose external fungal growth and then stained for 15 min in 2 mM Evans blue (Sigma-Aldrich) dissolved in 0.1 M $CaCl_2$ pH 5.6. Following, roots were washed extensively with ddH_2O for 1 hour and a Leica M165 FC microscope was used for imaging.

To quantify Evans blue staining intensity, ImageJ was used to invert the pictures, draw out individual roots and measure and compare mean grey values.

Extraradical colonization assays

To quantify extraradical colonization of *S. indica* on Arabidopsis, seed-inoculated plants were grown for 10 days. Inoculated and mock-treated seedlings were stained directly on plate by pipetting 2 ml of 1X PBS solution containing Alexa Fluor 488 conjugated with Wheat Germ Agglutinin (WGA-AF 488, Invitrogen). After 2 min of incubation, the roots were washed twice on the plate with 1X PBS solution. The stained seedlings were transferred to a fresh ½ MS plate and scanned with an Odyssey M Imaging System (LI-COR Biosciences) using brightfield and Alexa Fluor 488 channel. Quantification of WGA-AF 488 fluorescence was performed using EmpiriaStudio Software (LI-COR Biosciences).

RNA extraction (intraradical colonization assay)

For RNA extraction to measure intraradical colonization, plants were harvested at three time points around 7, 10 and 14 dpi. The roots were extensively wash with ddH_2O and tissue paper was used carefully wipe off external fungal colonization. The roots were shock frozen in liquid nitrogen and fungal and plant RNA was extracted with TRIzol (Invitrogen, Thermo Fisher Scientific, Schwerte, Germany). After a DNase I (Thermo Fisher Scientific) treatment according to the manufacturer's instructions to remove DNA, RNA was synthesized to cDNA using the Fermentas First Strand cDNA Synthesis Kit (Thermo Fisher Scientific).

Quantitative RT-PCR analysis

The quantitative real time-PCR (qRT-PCR) was performed using a CFX connect real time system (BioRad) with the following program: 95 °C 3min, 95 °C 15s, 59 °C 20s, 72 °C 30 s, 40 cycles and melting curve analysis. Relative expression was calculated using the $2^{-\Delta\Delta CT}$ method (Livak and Schmittgen 2001). qRT-PCR primers can be found in Table S1.

Filter trap analyses

Filter trap assays were performed as previously described (Llamas *et al.*, 2022, Llamas et al., 2021). Protein extracts were obtained using native lysis buffer (300 mM NaCl, 100 mM HEPES pH 7.4, 2 mM EDTA, 2% Triton X-100) supplemented with 1x plant protease inhibitor (Merck). Cell debris was removed by several centrifugation steps at 8,000 x *g* for 10 min at 4 °C. The supernatant was separated, and protein concentration determined using the Pierce BCA Protein Assay Kit (Thermo Fisher). A cellulose acetate membrane filter (GE Healthcare Life Sciences) and 3 filter papers (BioRad, 1620161) were immersed in 1x PBS and placed in a slot blot apparatus (Bio-Rad) connected to a vacuum system. The membrane was equilibrated by 3 washes with equilibration buffer (native buffer containing 0.5% SDS). 300, 200 and 100 µg of the protein extract were mixed with SDS at a final concentration of 0.5% and filtered through the membrane. The membrane was then washed with 0.2% SDS and blocked with 3% BSA in TBST for 30 minutes, followed by 3 washes with TBST. Incubation was performed with anti-polyQ [1:1000] (Merck, MAB1574). The membrane was washed 3 times for 5 min and incubated with secondary antibodies in TBST 3% BSA for 30 min. The membrane was developed using the Odyssey M Imaging System (LI-COR Biosciences). Extracts were also analyzed by SDS-PAGE and western blotting against anti-Actin [1:5000] (Agrisera, AS132640) to determine loading controls.

Confocal laser scanning microscopy (CLSM) and Proteostat staining quantification

CLSM images were acquired using either the FV1000 confocal laser scanning microscope (Olympus) or a Meta 710 confocal microscope with laser ablation 266 nm (Zeiss). All images were acquired using the same parameters between experiments. Excitation of WGA-AF 488 was done with an argon laser at 488 nm and the emitted light was detected with a hybrid detector at 500-550 nm. Proteostat was excited at 561 nm and the signal was detected between 590-700 nm. Hoechst was excited

with a diode laser at 405 nm and the emitted light was detected with a hybrid detector at 415-460 nm.

Proteostat staining

For the detection of aggregated proteins, we used the Proteostat Aggresome detection kit (Enzo Life Sciences). Seedlings were stained according to the manufacturer's instructions. Seedlings were incubated with permeabilizing solution (0.5% Triton X-100, 3 mM EDTA, pH 8.0) for 30 minutes at 4ºC with gentle shaking. The seedlings were washed twice with 1X PBS. Then the plants were incubated in the dark with 1x PBS supplemented with 0.5 µl/ml Proteostat and 0.5 µl/ml Hoechst 33342 (nuclear stain) for 30 min at room temperature. Finally, the seedlings were washed twice with 1x PBS and mounted on a slide for CLSM analysis or in mounted in fresh MS plates for LI-COR analysis. Quantification of Proteostat fluorescence was performed using Fiji software or EmpiriaStudio Software (LI-COR Biosciences).

Transcriptomic analysis

Arabidopsis Col-0 roots were inoculated with *S. indica*. Arabidopsis roots were harvested from mock plants and inoculated plants at three different time points after inoculation: 3, 6 and 10 dpi. Three biological replicates were considered for each condition. The RNA-seq libraries were generated and sequenced at US Department of Energy Joint Genome Institute (JGI) under a project proposal (Proposal ID: 505829) (Zuccaro & Langen, 2020). For each sample, stranded RNASeq libraries were generated and quantified by qRT-PCR. RNASeq libraries were sequenced with Illumina sequencer. Raw reads were filtered and trimmed using the JGI QC pipeline. Filtered reads from each library were aligned to the Arabidopsis genome (TAIR10) using HISAT2 (Kim *et al.*, 2015) and the reads mapped to each gene were counted using featureCounts (Liao *et al.*, 2014) Differential gene expression analysis was performed using the R package DESeq2 (Love *et al.*, 2014). Genes having aFDR adjusted p-value < 0.05 were considered as differentially expressed genes (DEGs).

CONTRIBUTIONS

Conceptualization: NC, EL, MN, AZ

Methodology: NC, EL, CDQ

Investigation: NC, EL, CDQ, DV, MN, AZ

Visualization: NC, EL, CDQ

Funding acquisition: MN, AZ

Project administration: AZ

Supervision: MN, AZ

Writing original draft: EL, NC, AZ

Writing review and editing: All authors

Acknowledgements

We thank the imaging facilities of CECAD (A. Schauss and C. Jüngst) and CEPLAS (P.S. Tan) for their assistance with CLSM. We thank Lisa Mahdi for conducting the experiments and providing the samples used for the RNA-seq analysis. We further would like to thank Yu Zhang, Sravanthi Tejomurthula, Daniel Peterson, Vivian Ng & Igor Grigoriev and their work performed in the work proposal (10.46936/10.25585/60001292) conducted by the U.S. Department of Energy Joint Genome Institute (https://ror.org/04xm1d337), a DOE Office of Science User Facility, is supported by the Office of Science of the U.S. Department of Energy operated under Contract No. DE-AC02-05CH11231.

Funding

German Research Foundation (DFG) - Excellence Strategy of the Federal Republic of Germany - EXC-2048/1 - project ID 390686111 (CEPLAS) (NC, EL, AZ)

German Research Foundation (DFG) - SFB-1403-414786233 (AZ)

German Research Foundation (DFG) - German Excellence Strategy-CECAD, EXC 2030-390661388 (DV).

Competing interests:

The Authors declare that they have no competing interests.

Data and materials availability:

All data are available in the main text or supplementary materials. Additional data/materials for this paper can be requested from the authors.

References

Barlow, P. W. (2002) The Root Cap: Cell Dynamics, Cell Differentiation and Cap Function. *Journal of Plant Growth Regulation,* **21,** 261-286.

Bennett, T., van den Toorn, A., Sanchez-Perez, G. F., Campilho, A., Willemsen, V., Snel, B.*, et al.* (2010) SOMBRERO, BEARSKIN1, and BEARSKIN2 regulate root cap maturation in Arabidopsis. *Plant Cell,* **22,** 640-654.

Boorboori, M. R. and Zhang, H. Y. (2022) The Role of Serendipita indica (Piriformospora indica) in Improving Plant Resistance to Drought and Salinity Stresses. *Biology (Basel),* **11**.

Cheng, J., Syder, A. J., Yu, Q. C., Letai, A., Paller, A. S. and Fuchs, E. (1992) The genetic basis of epidermolytic hyperkeratosis: a disorder of differentiation-specific epidermal keratin genes. *Cell,* **70,** 811-819.

Deshmukh, S., Huckelhoven, R., Schafer, P., Imani, J., Sharma, M., Weiss, M.*, et al.* (2006) The root endophytic fungus Piriformospora indica requires host cell death for proliferation during mutualistic symbiosis with barley. *Proc Natl Acad Sci U S A,* **103,** 18450-18457.

Dettmer, P. (2021) *Immune: The new book from Kurzgesagt - a gorgeously illustrated deep dive into the immune system*. Hodder & Stoughton.

Dolan, L., Janmaat, K., Willemsen, V., Linstead, P., Poethig, S., Roberts, K.*, et al.* (1993) Cellular organisation of the Arabidopsis thaliana root. *Development,* **119,** 71-84.

Dunken, N., Widmer, H., Balcke, G. U., Straube, H., Langen, G., Charura, N. M.*, et al.* (2022) A fungal endophyte-generated nucleoside signal regulates host cell death and promotes root colonization. *bioRxiv***,** 2022.2003.2011.483938.

Duxbury, Z., Wang, S., MacKenzie, C. I., Tenthorey, J. L., Zhang, X., Huh, S. U.*, et al.* (2020) Induced proximity of a TIR signaling domain on a plant-mammalian NLR chimera activates defense in plants. *Proc Natl Acad Sci U S A,* **117,** 18832-18839.

Escamez, S., Andre, D., Sztojka, B., Bollhoner, B., Hall, H., Berthet, B.*, et al.* (2020) Cell Death in Cells Overlying Lateral Root Primordia Facilitates Organ Growth in Arabidopsis. *Curr Biol,* **30,** 455-464 e457.

Farage-Barhom, S., Burd, S., Sonego, L., Perl-Treves, R. and Lers, A. (2008) Expression analysis of the BFN1 nuclease gene promoter during senescence, abscission, and programmed cell death-related processes. *J Exp Bot,* **59,** 3247-3258.

Fendrych, M., Van Hautegem, T., Van Durme, M., Olvera-Carrillo, Y., Huysmans, M., Karimi, M.*, et al.* (2014) Programmed cell death controlled by ANAC033/SOMBRERO determines root cap organ size in Arabidopsis. *Curr Biol,* **24,** 931-940.

Feng, Q., De Rycke, R., Dagdas, Y. and Nowack, M. K. (2022) Autophagy promotes programmed cell death and corpse clearance in specific cell types of the Arabidopsis root cap. *Curr Biol,* **32,** 2110-2119 e2113.

Fesel, P. H. and Zuccaro, A. (2016) Dissecting endophytic lifestyle along the parasitism/mutualism continuum in Arabidopsis. *Curr Opin Microbiol,* **32,** 103-112.

Heo, J. O., Blob, B. and Helariutta, Y. (2017) Differentiation of conductive cells: a matter of life and death. *Curr Opin Plant Biol,* **35,** 23-29.

552 Humphris, S. N., Bengough, A. G., Griffiths, B. S., Kilham, K., Rodger, S., Stubbs, V., *et*
553 *al.* (2005) Root cap influences root colonisation by Pseudomonas fluorescens
554 SBW25 on maize. *FEMS Microbiol Ecol,* **54,** 123-130.
555 Huysmans, M., Buono, R. A., Skorzinski, N., Radio, M. C., De Winter, F., Parizot, B., *et*
556 *al.* (2018) NAC Transcription Factors ANAC087 and ANAC046 Control Distinct
557 Aspects of Programmed Cell Death in the Arabidopsis Columella and Lateral
558 Root Cap. *Plant Cell,* **30,** 2197-2213.
559 Jacobs, S., Zechmann, B., Molitor, A., Trujillo, M., Petutschnig, E., Lipka, V., *et al.*
560 (2011) Broad-spectrum suppression of innate immunity is required for
561 colonization of Arabidopsis roots by the fungus Piriformospora indica. *Plant*
562 *Physiol,* **156,** 726-740.
563 Kim, D., Langmead, B. and Salzberg, S. L. (2015) HISAT: a fast spliced aligner with low
564 memory requirements. *Nat Methods,* **12,** 357-360.
565 Kumar, N. and Iyer-Pascuzzi, A. S. (2020) Shedding the Last Layer: Mechanisms of
566 Root Cap Cell Release. *Plants (Basel),* **9**.
567 Kumpf, R. P. and Nowack, M. K. (2015) The root cap: a short story of life and death. *J*
568 *Exp Bot,* **66,** 5651-5662.
569 Liao, Y., Smyth, G. K. and Shi, W. (2014) featureCounts: an efficient general purpose
570 program for assigning sequence reads to genomic features. *Bioinformatics,* **30,**
571 923-930.
572 Llamas, E., Koyuncu, S., Lee, H. J., Gutierrez-Garcia, R., Dunken, N., Charura, N., *et*
573 *al.* (2022) Chloroplast protein import determines plant proteostasis and
574 retrograde signaling. *bioRxiv***,** 2022.2003.2019.484971.
575 Llamas, E., Torres-Montilla, S., Lee, H. J., Barja, M. V., Schlimgen, E., Dunken, N., *et*
576 *al.* (2021) The intrinsic chaperone network of Arabidopsis stem cells confers
577 protection against proteotoxic stress. *Aging Cell,* **20,** e13446.
578 Love, M. I., Huber, W. and Anders, S. (2014) Moderated estimation of fold change and
579 dispersion for RNA-seq data with DESeq2. *Genome Biol,* **15,** 550.
580 Mahdi, L. K., Miyauchi, S., Uhlmann, C., Garrido-Oter, R., Langen, G., Wawra, S., *et al.*
581 (2022) The fungal root endophyte Serendipita vermifera displays inter-kingdom

synergistic beneficial effects with the microbiota in Arabidopsis thaliana and barley. *ISME J,* **16,** 876-889.

Moriwaki, T., Miyazawa, Y., Kobayashi, A. and Takahashi, H. (2013) Molecular mechanisms of hydrotropism in seedling roots of Arabidopsis thaliana (Brassicaceae). *Am J Bot,* **100,** 25-34.

Olvera-Carrillo, Y., Van Bel, M., Van Hautegem, T., Fendrych, M., Huysmans, M., Simaskova, M.*, et al.* (2015) A Conserved Core of Programmed Cell Death Indicator Genes Discriminates Developmentally and Environmentally Induced Programmed Cell Death in Plants. *Plant Physiol,* **169,** 2684-2699.

Reza, S. H., Delhomme, N., Street, N. R., Ramachandran, P., Dalman, K., Nilsson, O.*, et al.* (2018) Transcriptome analysis of embryonic domains in Norway spruce reveals potential regulators of suspensor cell death. *PLoS One,* **13,** e0192945.

Shi, C. L., von Wangenheim, D., Herrmann, U., Wildhagen, M., Kulik, I., Kopf, A.*, et al.* (2018) The dynamics of root cap sloughing in Arabidopsis is regulated by peptide signalling. *Nat Plants,* **4,** 596-604.

Vijayaraghavareddy, P., Adhinarayanreddy, V., Vemanna, R. S., Sreeman, S. and Makarla, U. (2017) Quantification of Membrane Damage/Cell Death Using Evan's Blue Staining Technique. *Bio Protoc,* **7,** e2519.

Weiss, M., Waller, F., Zuccaro, A. and Selosse, M. A. (2016) Sebacinales - one thousand and one interactions with land plants. *New Phytol,* **211,** 20-40.

Willemsen, V., Bauch, M., Bennett, T., Campilho, A., Wolkenfelt, H., Xu, J.*, et al.* (2008) The NAC domain transcription factors FEZ and SOMBRERO control the orientation of cell division plane in Arabidopsis root stem cells. *Dev Cell,* **15,** 913-922.

Yu, D., Song, W., Tan, E. Y. J., Liu, L., Cao, Y., Jirschitzka, J.*, et al.* (2022) TIR domains of plant immune receptors are 2',3'-cAMP/cGMP synthetases mediating cell death. *Cell,* **185,** 2370-2386 e2318.

Zuccaro, A., Lahrmann, U., Guldener, U., Langen, G., Pfiffi, S., Biedenkopf, D.*, et al.* (2011) Endophytic life strategies decoded by genome and transcriptome analyses of the mutualistic root symbiont Piriformospora indica. *PLoS Pathog,* **7,** e1002290.

613 Zuccaro, A. and Langen, G. (2020) Host-specific regulation of effector gene expression
614 in mutualistic root endophytic fungi (Proposal ID: 505829). JGI Award

615

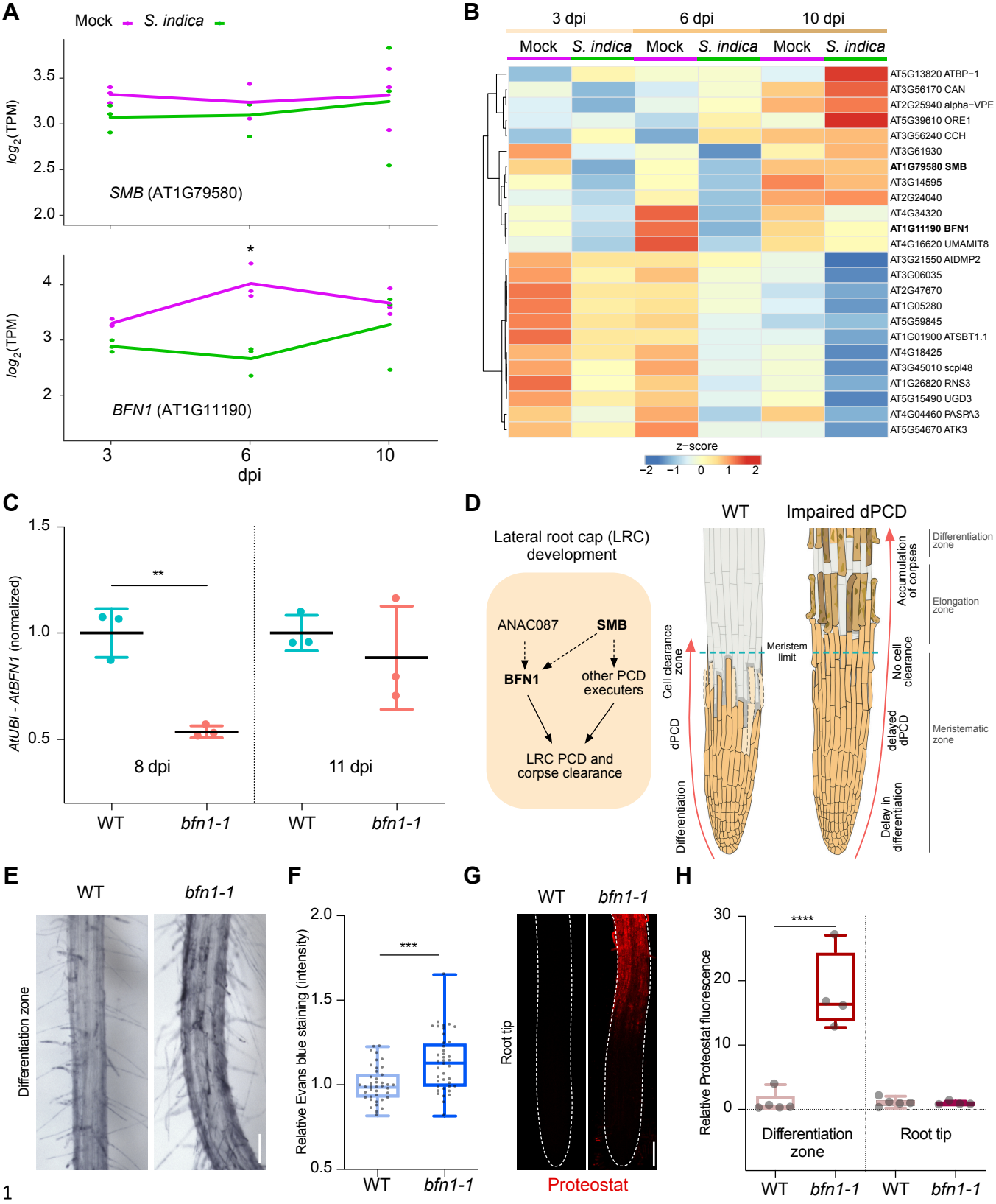

Figure 1. *BFN1* is downregulated during interaction with *S. indica*. (A) Expression profiles of *SMB* and *BFN1* genes in Arabidopsis roots mock-treated or inoculated with *S. indica* at 3, 6 and 10 dpi. The log_2-transformed TPM values are shown and the lines indicate the average expression values among the 3 biological replicates. Asterisk indicates significantly different expression (adjusted p-value < 0.05) (B) The heat map shows the expression values (TPM) of Arabidopsis dPCD marker genes with at least an average of 1 TPM across Arabidopsis roots mock-treated or inoculated with *S. indica* at 3, 6 and 10 dpi. The TPM expression values are log_2 transformed and row-scaled. Genes are clustered using spearman correlation as distance measure. The dPCD gene markers were previously defined (Olvera-Carrillo *et al.*, 2015). (C) *BFN1* expression in WT Arabidopsis during *S. indica* colonization at 8 and 11 dpi. RNA was isolated from 3 biological replicates for qRT-PCR analysis, comparing *BFN1* expression with an Arabidopsis ubiquitin marker gene. (D) Schematic representation of lateral root cap (LRC) development in WT and in mutant plants impaired in dPCD. (E) Representative images of the differentiation zone of 14-day-old WT and *bfn1-1* roots, stained with Evans blue. Scale indicates 100 µm. (F) Quantification of Evans blue staining, comparing 14-day-old WT and *bfn1-1* roots. 10 plants were used for each genotype, taking 4 pictures along the main root axis per plant. ImageJ was used to calculate the mean grey value to compare relative staining intensity. Statistical significance was determined using an unpaired, two-tailed Student's t test before normalization (*** $P < 0.0001$). (G) Representative Proteostat staining images of 10-day-old WT and *bfn1-1* root tips. Scale indicates 100 µm. (H) Quantification of Proteostat staining using 4 to 5 10-day-old WT and *bfn1-1* roots. Statistical analysis was performed via one-way ANOVA and Tukey's post hoc test before normalization (significance threshold: $P \leq 0.05$).

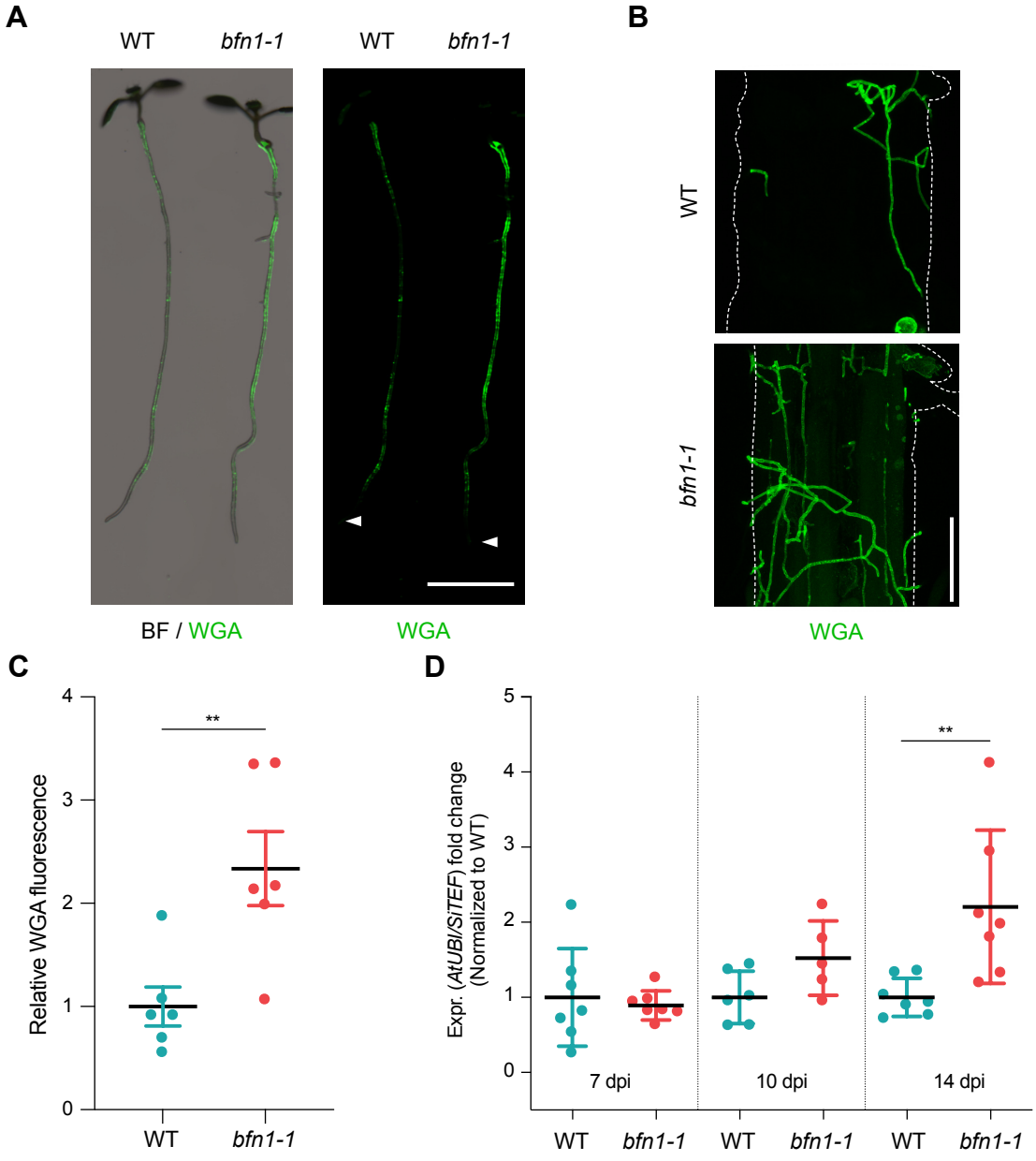

Figure 2. *bfn1-1* roots show increased colonization by *S. indica*. (A) Representative images show extraradical colonization of 10-day-old WT and *bfn1-1* plants, seed-inoculated with *S. indica*. The fungus was stained with WGA-AF 488. Roots were scanned and captured with a LI-COR Odyssey M imager using the bright field (BF) and Alexa Fluor 488 channel. Arrowheads indicate the position of the root tips. Scale indicates 5 mm. (B) Representative images of Arabidopsis WT and *bfn1-1* roots inoculated with *S. indica* obtained by CLSM. The fungus was stained with WGA-AF 488. Scale represents 50 µm. (C) Relative quantification of WGA-AF 488 signal as a proxy for extra-radical colonization of *bfn1-1* and WT roots. Statistical comparisons were made by unpaired, two-tailed Student's t test for unpaired samples (**$P < 0.01$) (D) Quantitative RT-PCR analysis to measure intraradical *S. indica* colonization in WT and *bfn1-1* roots. Roots were collected from 3 biological replicates, using approximately 30 plants per time point and replicate for each genotype. Each time point in the graph is normalized to WT for relative quantification of colonization. Statistical analysis was performed via one-way ANOVA and Tukey's post hoc test (significance threshold: $P \leq 0.05$).

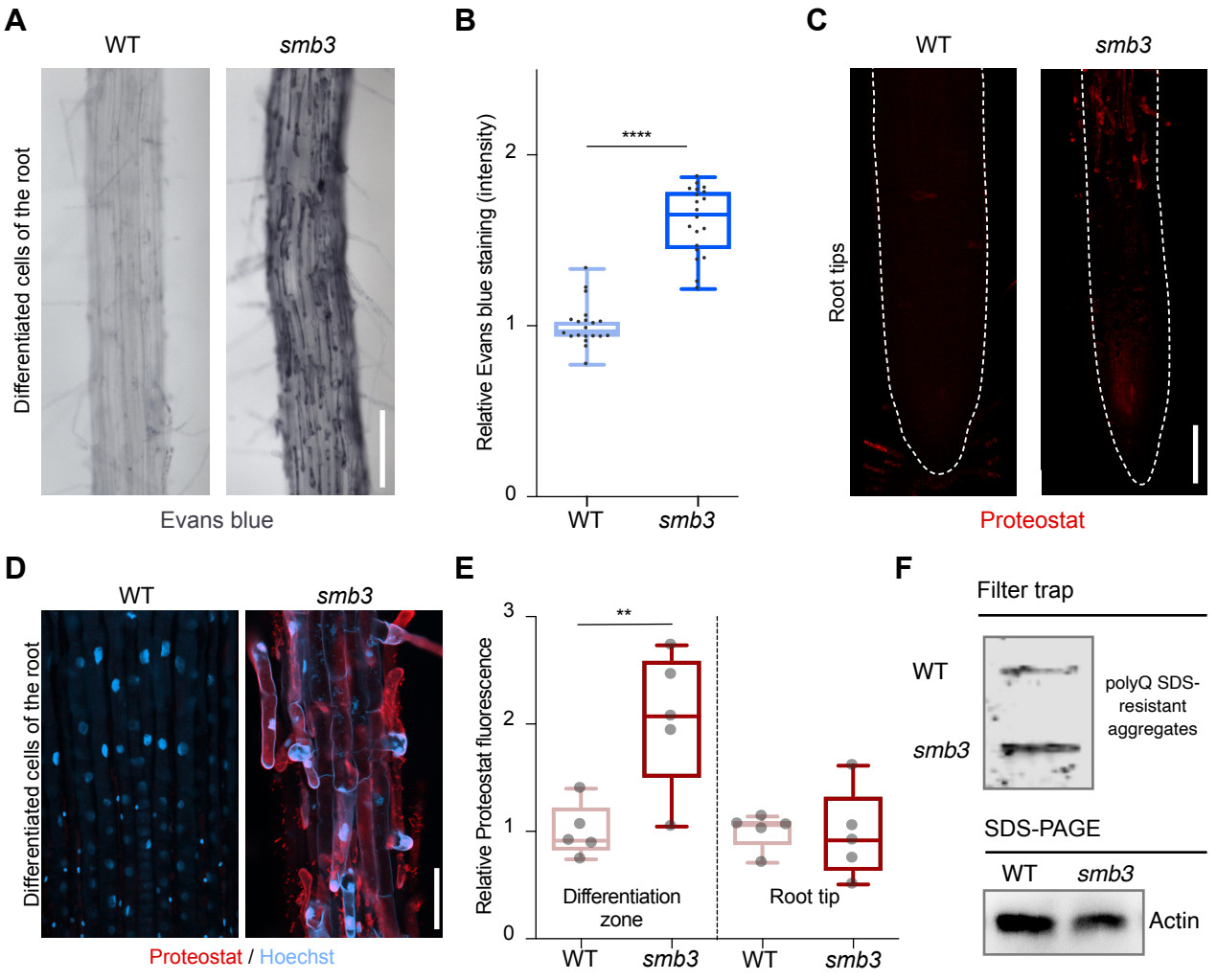

Figure 3. *smb3* roots exhibit uncleared cell corpses loaded with misfolded / aggregated proteins. (A) Evans blue staining of the differentiation zone in 17-day-old WT and *smb3* roots. Scale indicates 100 µm. (B) Relative quantification of Evans blue staining of the differentiation zone in 14-day-old WT and *smb3* roots. 5 plants per genotype were used, taking 4 images per plant along the main root axis. Statistical relevance was determined by unpaired, two-tailed Student's t test before normalization (****$P < 0.0001$). (C) Representative images of 10-day-old WT and *smb3* roots stained with Proteostat (red). Scale indicates 100 µm. (D) Magnification of the differentiation zone of WT and *smb3* roots. Proteostat (red) and Hoechst (blue) channels are shown. Scale indicates 50 µm. (E) Quantification of relative Proteostat fluorescence levels comparing the differentiation and meristematic zones of WT and *smb3*. 5 x 10-day-old plants were used for each genotype. Statistical significance was determined by one-way ANOVA and Tukey's post hoc test before normalization (significance threshold: $P \leq 0.05$). (F) Filter trap and SDS-PAGE analysis with antibody against poly-glutamine (polyQ) regions of 15-day-old WT and *smb3* roots. The images are representative of two independent experiments.

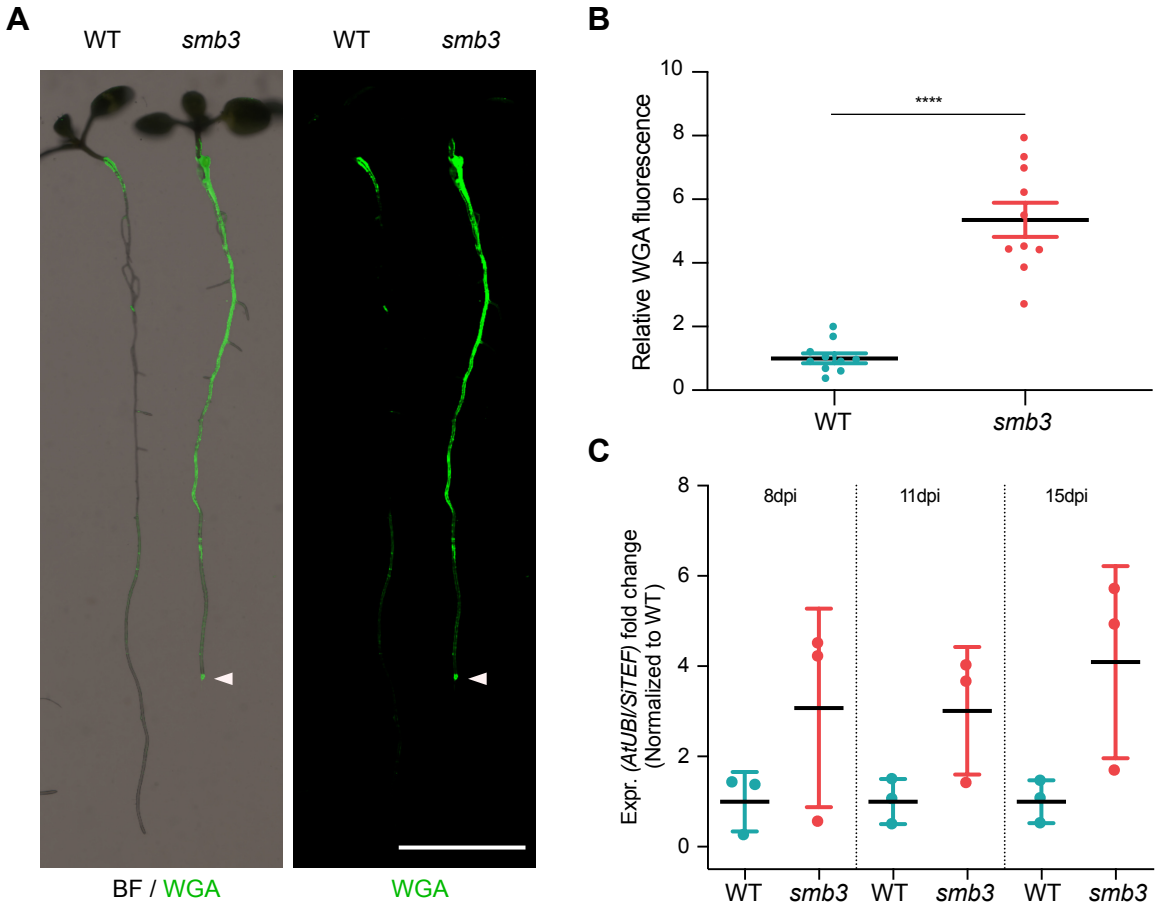

Figure 4. *smb3* roots display increased intra- and extraradical colonization by *S. indica*. (A) Representative image showing extraradical colonization of 10-day-old WT and *smb3* seedlings (seed inoculated). *S. indica* was stained with WGA-AF 488. Roots were scanned and captured with a LI-COR Odyssey M imager using the bright field (BF) and Alexa Fluor 488 channel. White arrowheads indicate colonization at the root tip in *smb3*. Scale indicates 5 mm. (B) Relative quantification of WGA-AF 488 signal indicating extraradical colonization on *smb3* and WT roots. The statistical comparison was made by two-tailed Student's t test for unpaired samples (****$P < 0.0001$) using 10 plants. (C) Measurement of intraradical colonization in WT and *smb3* roots performed by quantitative RT-PCR. Roots from 3 biological replicates were collected and washed to remove extraradical hyphae, using approximately 30 seedlings for each genotype per time point and replicate. Each time point in the graph is normalized to WT for a relative quantification of colonization. Statistical analysis was done via one-way ANOVA and Tukey's post hoc test after normalization (significance threshold: $P \leq 0.05$).

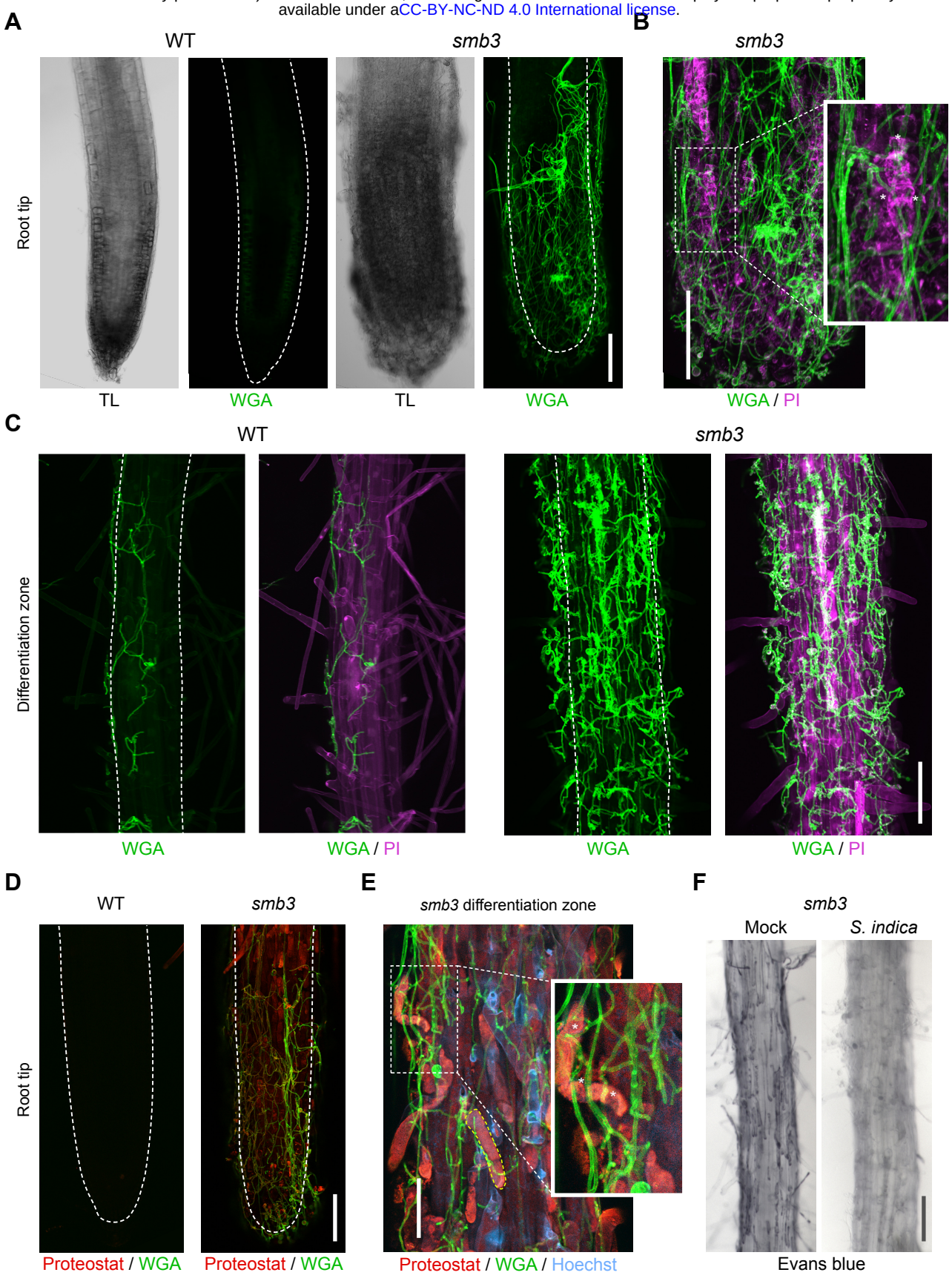

Figure 5. Cytological analysis of *S. indica*-colonized *smb3* and WT roots. For microscopic analysis, 7-day-old seedlings were inoculated with *S. indica* spores and the roots were analyzed at 10 dpi. (A) Representative images of Arabidopsis WT and *smb3* roots inoculated with *S. indica*. *S. indica* was stained with WGA-AF 488. Transmitted light (TL) images are also shown. Scale indicates 100 µm (B) Magnification of *smb3* root tip colonized with *S. indica*. Asterisks indicate penetration of hyphae stained with WGA-AF 488 into dead cells stained with propidium iodide (PI). Scale indicates 100 µm. (C) Representative images of WT and *smb3* roots colonized with *S. indica* and stained with WGA-AF 488 and PI. Scale indicates 100 µm. (D) Representative images of WT and *smb3* root tips inoculated with *S. indica* stained with WGA-AF 488 and Proteostat. Scale indicates 100 µm (E) Magnification of *smb3* root differentiation zone showing *S. indica* colonization stained with WGA-AF 488, Hoechst and Proteostat. Penetration of uncleared cell corpses is marked with asterisks. Dotted yellow line indicates LRC cell corpse. Scale indicates 50 µm. (F) Evans blue staining showing sections of the differentiation zone in *smb3* mock-treated and colonized roots with *S. indica* at 10 dpi**.** Scale indicates 100 µm.

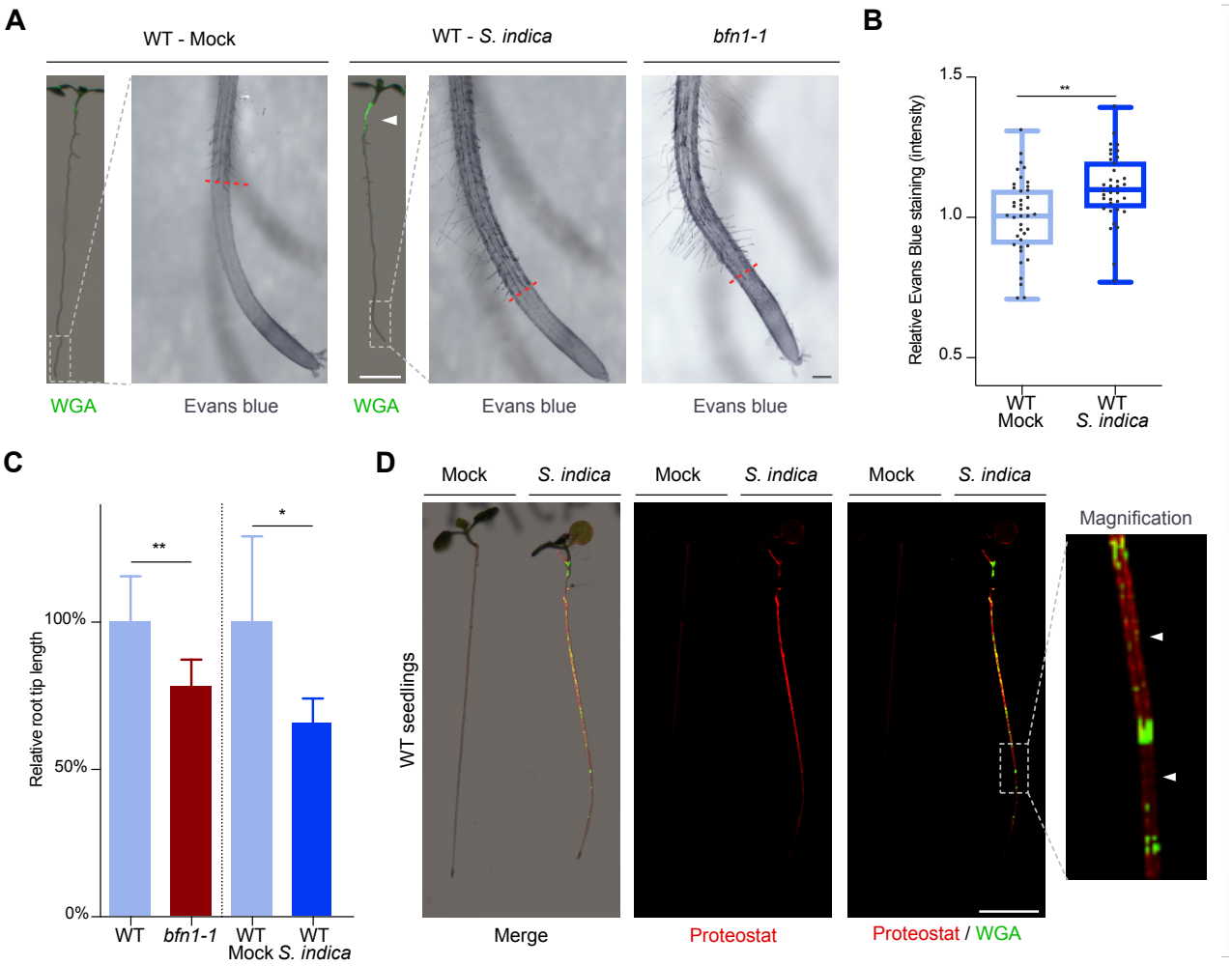

Figure 6. *S. indica* causes a systemic cell death response in the root differentiation zone. (A) Comparison between *S. indica*-inoculated WT roots and *bfn1-1*. Representative images show whole plant scans taken with LI-COR and microscopy overviews of the root tip. The LI-COR scans of fungal mycelium stained with WGA-AF 488 show a preference for the mature differentiation zone for fungal colonization, indicated by a white arrowhead. Scale bar indicates 5 mm. Evans blue cell death staining in WT-mock, WT-colonized, and *bfn1-1* roots highlights a pattern of dead cells in the *bfn1-1* mutant and *S. indica*-colonized WT at the onset of the differentiated tissue as indicated with dotted red lines. Scale bar indicates 100 µm. (B) Quantification of *S. indica* induced cell death in WT Arabidopsis, measuring relative Evans blue staining intensity. 10 plants at 6dpi were used, taking 4 images along the main root of each plant. Statistical evaluation was performed with a two-tailed Student's t test for unpaired samples (**P = 0.0011). (C) To determine relative root tip length in WT Arabidopsis, *bfn1-1* mutant and *S. indica*-colonized WT plants, the distance from the tip of the root to the first root hair, representing the start of the differentiation zone was measured. For this analysis 2 different datasets were analyzed, the first one representing 10 14-day-old WT and *bfn1-1* plants and the second showing 6 *S. indica*-colonized WT plants and their mock counterpart at 12dpi. For both datasets, WT mock was set to 100% root length. Statistical evaluation was performed by two-tailed Student's t test for unpaired samples (**P < 0.0012 for bfn1-1 and *P = 0.033 for *S. indica*-

inoculated WT). (D) Representative Proteostat images of *S. indica*-colonized WT roots. Magnification panel shows Proteostat staining in zones of the root where *S. indica* is not present (white arrowheads). Scale indicates 5 mm.

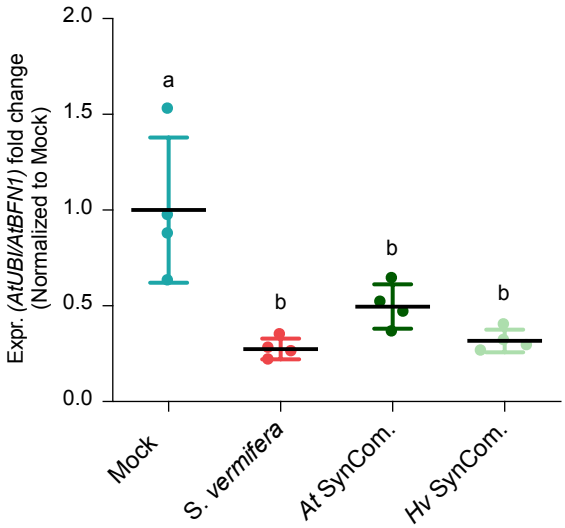

Figure 7. *BFN1* is downregulated during colonization by beneficial microbes. qRT-PCR shows downregulation of *BFN1* in *A. thaliana* (*At*) during colonization by *S. vermifera* and the *H. vulgare* (*Hv*) and *A. thaliana* bacterial SynComs. RNA was harvested from 4 replicates at 6 dpi using 30 plants per replicate for each treatment. *BFN1* expression levels are normalized to mock conditions. Statistical evaluation was performed via one-way ANOVA and Tukey's post hoc test before normalization (significance threshold: $P \leq 0.05$).

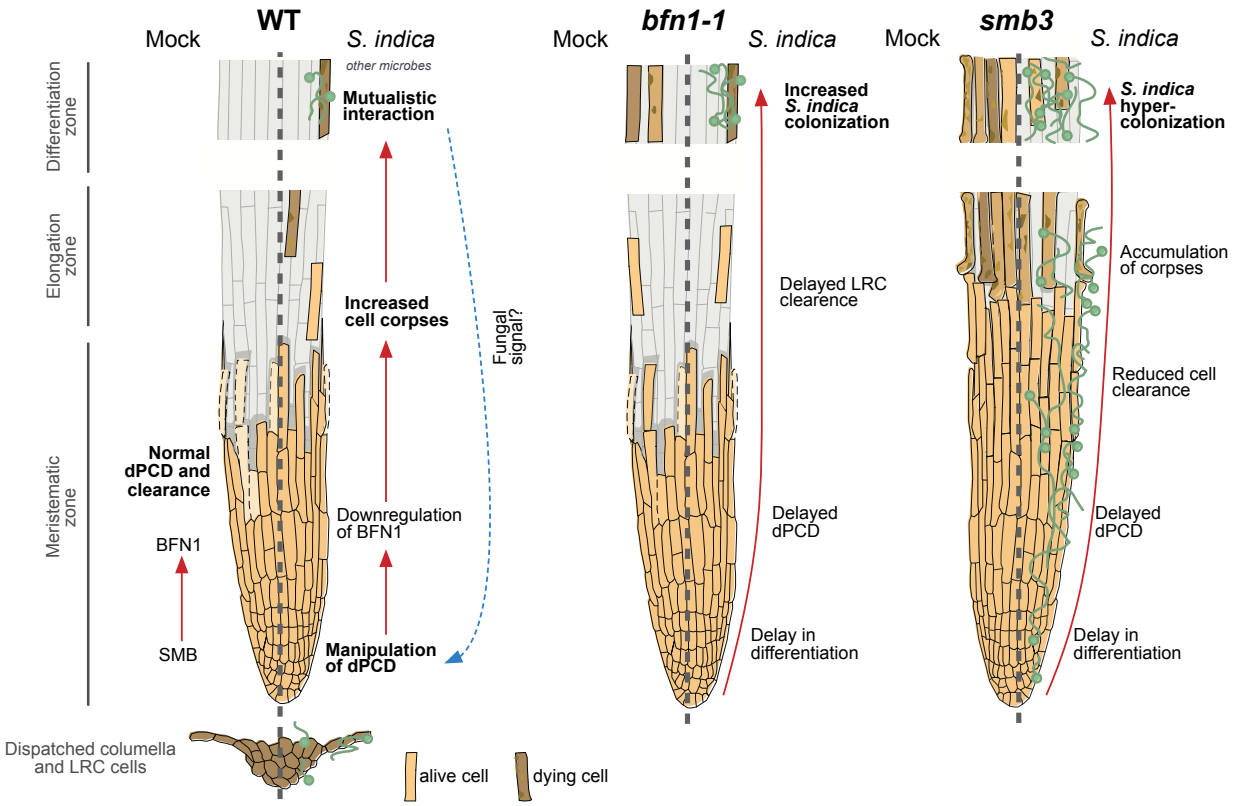

Figure 8. Proposed models for manipulation of dPCD and implications for the interaction with *S. indica*. The size of the root cap organ in Arabidopsis is maintained by high cell turnover of root cap cells and cell corpse clearance. While the columella root cap is shed from the root tip, a dPCD machinery marks the final step of LRC differentiation and prevents LRC cells from entering the elongation zone. Induction of cell death by the transcription factor SMB is followed by irreversible DNA fragmentation and cell corpse clearance, mediated by the nuclease BFN1, a downstream component of dPCD (Fendrych et al., 2014). The absence of dPCD induction in the *smb3* knockout mutant leads to a delay in LRC differentiation and allows LRC cells to enter the elongation zone, where they die uncontrolled and remain attached to the root as dying cells or cell corpses. The *smb3* phenotype results in hypercolonization of Arabidopsis by *S. indica*, as the fungus colonizes the entire root from the root tip to the differentiation zone and is not restricted to the differentiation zone as is the WT Arabidopsis roots. *S. indica* is capable of clearing the LRC cell corpses on *smb3*. During colonization, *S. indica* downregulates *BFN1* in Arabidopsis WT roots. We hypothesize that this leads to a reduced rate of cell corpse clearance in the root cap, which is beneficial for fungal colonization through increased nutrient availability in the form of dying LRC cells. Interestingly, the cell death pattern of *bfn1-1* mock roots and WT colonized roots are similar, indicating the importance of *BFN1* downregulation to manipulate plant dPCD pathways during plant-microbe interactions.